SOL-GEL PROCESSING AND PROPERTIES OF Eu^{3+} DOPED SiO_2 - B_2O_3 GLASSES

Hristo Lalkovski[1,2], Lyubomir Aleksandrov[1], Dessislava Mutafchieva[2], Albena Bachvarova - Nedelcheva[1]

[1]*Institute of General and Inorganic Chemistry, Bulgarian Academy of Sciences Acad. G. Bonchev St., Bl. 11, Sofia 1113 Bulgaria, lubomir@svr.igic.bas.bg (L.A.); lalkovski@svr.igic.bas.bg (H.L.); albenadb@svr.igic.bas.bg (A.B.-N.)*
[2]*Department of Engineering Chemistry, University of Chemical Technology and Metallurgy 8 Kliment Ohridski Blvd., Sofia 1797, Bulgaria, dmoutaf@uctm.edu (D.M.)*

Received 19 December 2025
Accepted 19 March 2026 *DOI: 10.59957/jctm.v61.i3.2026.11*

ABSTRACT

Eu^{3+} doped glasses from the SiO_2 - B_2O_3 system containing up to 20 mol % B_2O_3 have been synthesized. To obtain a homogeneous glass, it was determined that a certain degree of hydrolysis of $Si(OC_2H_5)_4$ was essential before $B(OC_2H_5)_3$ could be incorporated. These glasses have been characterized by X - ray diffraction, DTA and IR spectroscopy. According to the XRD method, amorphous gels have been obtained. IR spectra exhibited bands in the 1700 - 620 cm^{-1} range which could be related to the vibrations of SiO_4 and BO_3 inorganic structural units. Characteristic emission peaks of Eu^{3+} ions were detected in the luminescence spectra. The obtained results confirmed that Eu^{3+} doped glasses are useful for optical applications.

Keywords: *sol - gel, powders, luminescence, properties.*

INTRODUCTION

The sol - gel process offers a high degree of structural and compositional uniformity, making it a desirable synthetic route for developing advanced catalytic materials based on metals and metal oxides. It was first introduced by Ebelman in the mid-nineteenth century has been widely developed in the past century for usage in fibers, glasses, ceramics, catalysts, coatings, composites, and construction materials [1]. In recent decades sol - gel chemistry has been used to synthesize different materials due to its several advantages in comparison with traditional methods. This method is better controllable, using lower temperature and yielding a structure with better composition homogeneity along with uniform distribution of large amounts of dopants in the glass host matrix [2].

Unlike conventional methods, the sol - gel technique employs a low temperature synthesis route that provides precise control over the final microstructure. This approach enables the preparation of porous materials in a single "one - pot" process, ensuring a uniform atomic - scale distribution of the components. A gel is defined as an interconnected network of solid-phase particles forming a continuous structure within a secondary, usually liquid, phase. In contrast, a sol consists of a colloidal dispersion of solid particles. These two states represent the fundamental phases involved in sol - gel chemistry [3 - 5]. The sol - gel method offers several advantages, including high yields, low processing temperatures, and reduced production costs. Moreover, this synthesis route provides unique benefits, particularly the ability to tailor the physicochemical properties of the resulting materials by carefully adjusting the parameters involved in each step of the process. It is well established that sol - gel techniques offer several advantages, including low processing temperatures, low production costs, and excellent product yield. Moreover,

by carefully adjusting the parameters that influence each stage of the synthesis, the sol - gel technique enables precise control over the physicochemical properties of the resulting materials.

The sol - gel process is widely regarded as a form of "soft chemistry", distinguishing it from conventional industrial methods for producing glass and ceramic materials, which typically require high temperatures. Today, the term is broadly used to describe the synthesis of solid materials, especially metal oxides, from solution - based precursors [6 - 11] and has been extensively reviewed in the literature [2, 7, 9, 11].

For several years, researchers have been studying and using rare earth - doped glasses in a range of optical applications, including solid state lasers, fluorescent devices, white light emitting diodes (LEDs), plasma display panels (PDPs), and optical fiber amplifiers [12, 13]. Due to their outer - shell electrons of half - filled f orbital, rare earth ions can provide unique optical characteristics in glass matrices [14]. However, clustering could result from high rare earth doping levels. Both the luminescent characteristics and the irradiative combination are quenched by clustering [15, 16].

In this paper, SiO_2 - B_2O_3 glasses doped with Eu^{3+} were synthesized through sol - gel method and the influence of the glass matrix on the thermal and structural properties were studied.

EXPERIMENTAL

Preparation of the sol - gel glasses

In this study, two compositions from the SiO_2 - B_2O_3 system were investigated. The main used precursors were $Si(OC_2H_5)_4$ (Sigma - Aldrich), $B(OCH_2CH_3)_3$ (Triethyl borate) (Merck KGaA, Germany), $Eu(NO_3)_3 \cdot 5H_2O$ (Sigma - Aldrich). The hydrolysis, polymerization, and gelling were completed in about 18h. The gel was initially dried at room temperature for several days.

The batch formulations used for preparing the compositions are presented in Table 1. In the first stage of the synthesis, the $Si(OC_2H_5)_4$ was hydrolysed with predetermined amounts of water, HCl, and C_2H_5OH. After 1h, $B(OC_2H_5)_3$ was added to the batch along with the Eu^{3+} solution.

The dissolving in alcohol was performed by vigorous magnetic stirring. Homogeneous and transparent gels were obtained. The measured pH during the experiments was about 4 - 5. The detailed representation of the experimental procedure is shown in Fig. 1.

Samples characterization

Powder XRD patterns were registered at room temperature with a Bruker D8 Advance X - ray powder diffractometer with a Cu Ka radiation (k = 1.54056 A˚) with a LynxEye solid position sensitive detector and X - ray tube operated at 40 kV and 40 mA. X - ray diffraction patterns were recorded in the range of 5.3 - 80° 2h with a step of 0.02° 2h. The differential thermal analysis (LabSys EVO apparatus, Setaram, Lyon, France) with Pt - Pt/Rh thermocouple at a heating rate of 10 K min^{-1} in air flow and Al_2O_3 as a reference material was used to study the decomposition process of the gels. The accuracy of the temperature was ± 5°C. The IR spectra were registered in the range 1600 - 400 cm^{-1} using the KBr pellet technique on a Nicolet - 320 FT-IR spectrometer (Madison, USA) with 64 scans and a resolution of ± 1 cm^{-1}.

Optical microscopy images were recorded using a Light microscope BOECO, Boeckel & Co. GmbH & Co. KG, Hamburg, Germany, at magnification of 5 × and a transmission optical microscope ZEISS Primo Star, Carl Zeiss Microscopy GmbH, Jena, German at a magnification of 10 ×. Luminescence emission spectra at room temperature were measured with a high - resolution

Table 1. Nominal compositions of the investigated samples.

Gel abbreviation	Composition					
	SiO_2		B_2O_3		Eu_2O_3	
	mol %	wt %	mol %	wt %	mol %	wt %
80Si/B/Eu	80 %	75.81 %	19.5 %	21.41 %	0.5 %	2.78 %
90Si/B/Eu	90 %	86.59 %	9.5 %	10.59 %	0.5 %	2.82 %

spectrometer (Ocean Insight HR2000+), using a UV LED light sources at 385 nm as a typical absorption value for the Eu^{3+} ions. Both investigated samples were denoted as 90Si/B/Eu and 80Si/B/Eu.

RESULTS AND DISCUSSION

XRD and DTA results

The XRD patterns of as - prepared gels are presented in Fig. 2. As it is seen from the figure, both samples exhibited presence of an amorphous halo but the sample containing higher B_2O_3 amount showed typical diffraction lines of H_3BO_3 (ICDD 09 - 0062). These results well correspond to those obtained by Kumar [17].

The thermal behaviour was investigated using differential thermal analysis (DTA) with thermogravimetry (TG), from room temperature to 850°C (Fig. 3). Endothermic peaks in the range 100 - 150°C were observed in the DTA curves of both samples. These peaks are accompanied by a strong mass loss

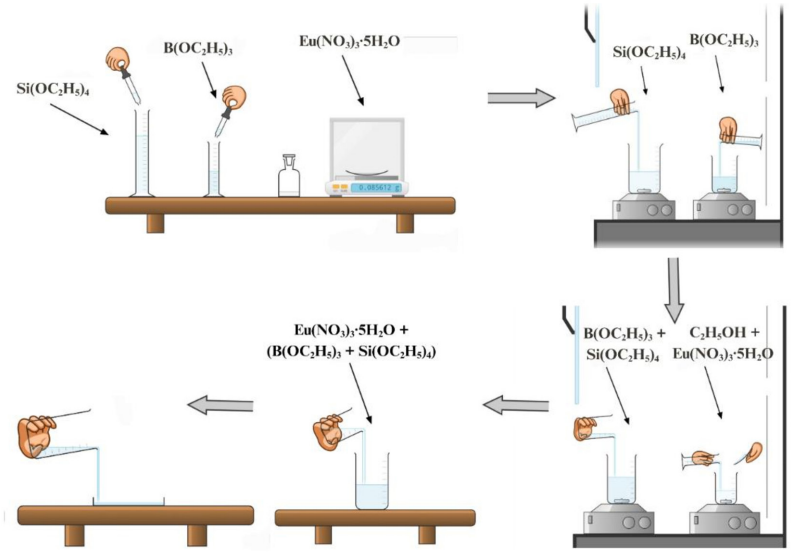

Fig. 1. Scheme for the synthesis of Eu^{3+} doped SiO_2/B_2O_3 gels.

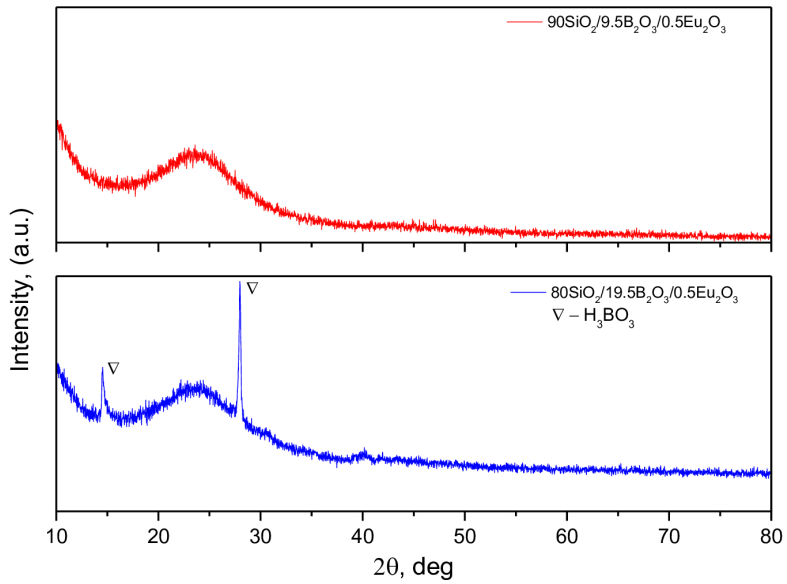

Fig. 2. XRD patterns of the investigated samples.

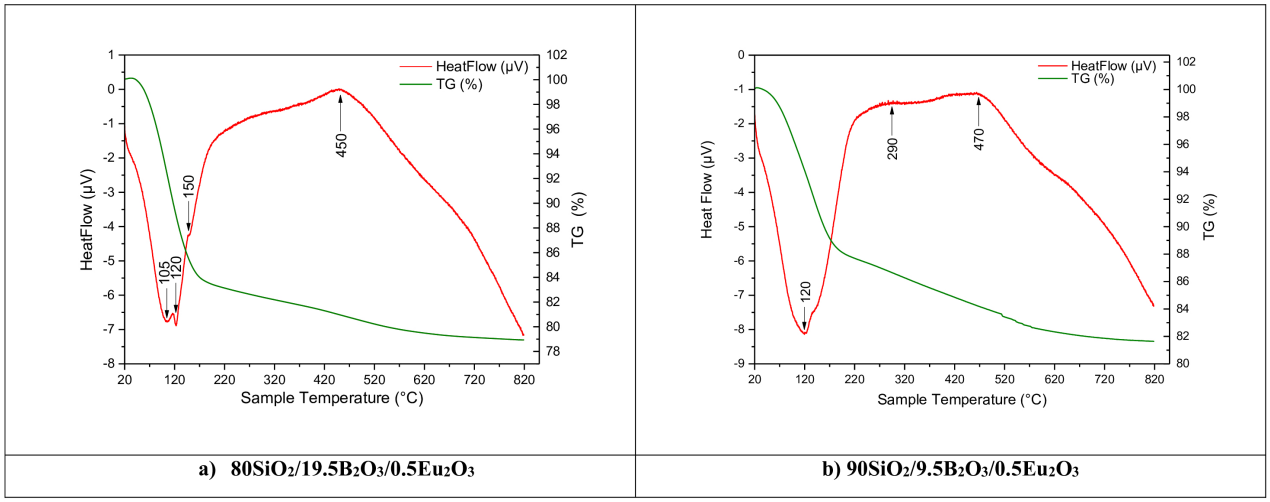

a) $80SiO_2/19.5B_2O_3/0.5Eu_2O_3$ b) $90SiO_2/9.5B_2O_3/0.5Eu_2O_3$

Fig. 3. DTA - TG curves of the investigated gels.

which confirmed the presence of absorbed water in the gels. No more endothermic effects were observed in the samples. Two exothermic effects were registered at 290 and 450°C that are accompanied by a decrease of the mass loss. This could be related to the decomposition of the tetraethoxysilane which cause the decrease of the weight to the gel powders [18].

Morphological characterizations of the sol - gel glasses

The microscope reflection images of the surface of the obtained sol - gel glasses are presented in Fig. 4. Both samples are characterized by a typical amorphous structure.

IR spectroscopy

The IR structural investigations in the range 1600 - 400 cm^{-1} are presented in Fig. 5. It is known that in sol - gel derived materials, the 3200 - 3500 cm^{-1} region is typically dominated by broad and overlapping bands associated with hydroxyl groups, adsorbed water, and hydrogen bonding. These contributions often overlap significantly and do not provide clear structural information about the network - forming units. That is why the discussion of the IR spectra was focused on the fingerprint region (400 - 1600 cm^{-1}), where the characteristic vibrations of the structural units forming the amorphous network are located and can be more reliably interpreted. As it is seen from the figure, the IR spectrum of sample 80Si/B/Eu that contains higher B_2O_3 content (19.5 mol %) exhibited absorption bands which are absent in the spectrum of 90Si/B/Eu sample. The main bands which are seen in both IR spectra are centered at 1400, 1200, 1100, 1000, 800, 550 and 450 cm^{-1}. These peaks could be divided to three regions: 1500 - 1100 cm^{-1}, 1000 - 800 cm^{-1} and 650 - 450 cm^{-1}. In the low frequency region, a well - defined band at 450 cm^{-1} is seen that is related to the Si - O - Si bending vibrations in the SiO_4 tetrahedra [19 - 22]. The bands at 650 and 550 cm^{-1} are observed in both spectra, but they are more pronounced in the spectrum of sample rich in B_2O_3 (19.5 mol %). Several authors stated that the bands at 650 and 550 cm^{-1} could be related to the bending vibrations of BO_3 trigonal units present in the structure of boric acid [23, 24]. This finding correlates well with our XRD results, as H_3BO_3 was registered in the sample 80Si/B/Eu, only.

In the second frequency region 1000 - 800 cm^{-1}, three absorption bands are distinguished. The bands at 1000 and 800 cm^{-1} are common for both IR spectra. These broad bands are related to the presence of Si - O - Si bonds in SiO_4 tetrahedra. A weak shoulder at about 670 cm^{-1} and the band at 900 cm^{-1} are observed in the spectra of sample 80Si/B/Eu, only, that could be connected to the higher B_2O_3 presence. The fact that there does not appear any absorption band in the gels around 720 cm^{-1} (B - O - B deformation vibration) [25, 26] and that the intensity of the bands corresponding to the stretching vibration (~ 900 cm^{-1}) and deformation vibration (670 cm^{-1}) of the Si - O - B links appeared with the increase of B_2O_3 content in the samples, suggests that all the B_2O_3

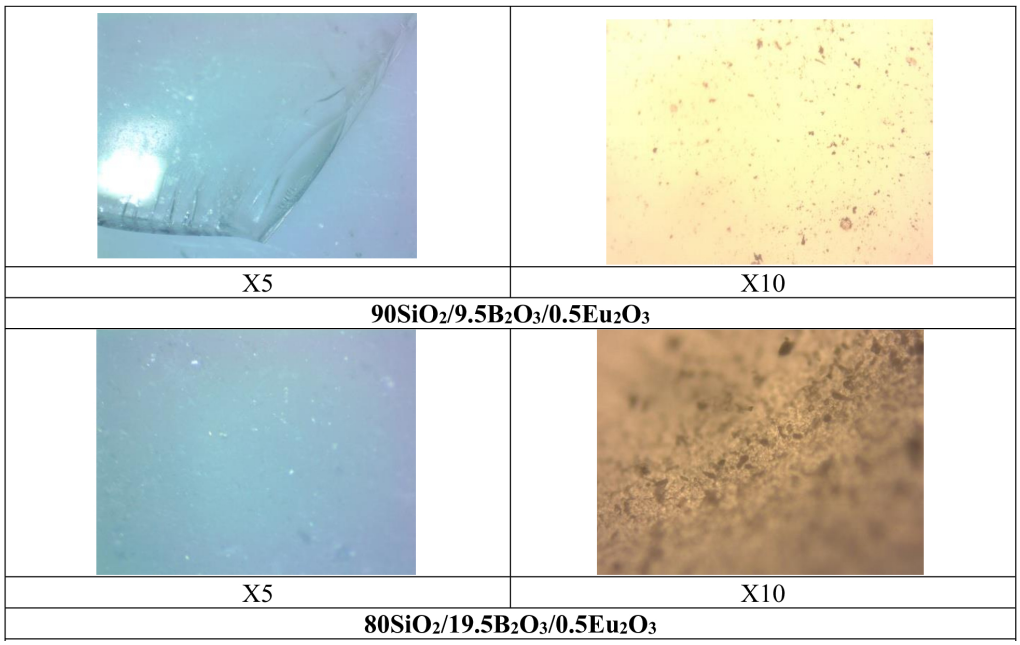

Fig. 4. Optical microscopy images on the investigated samples at different magnifications.

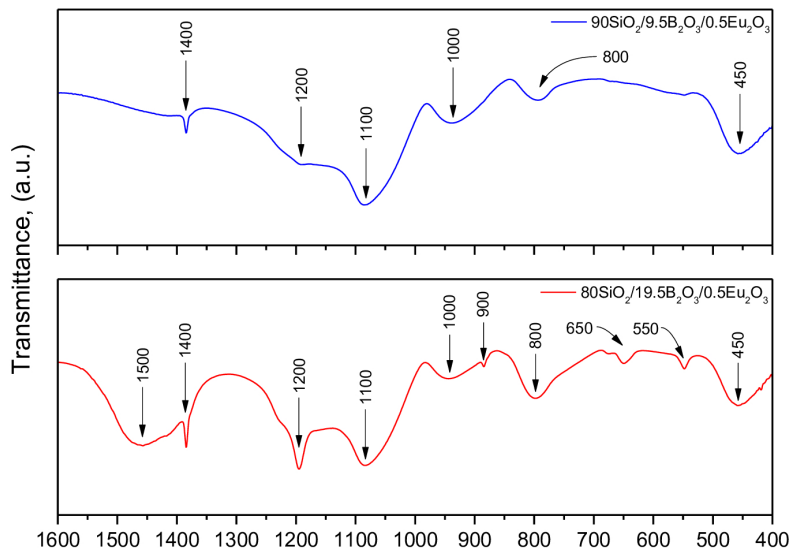

Fig. 5. IR spectroscopy of as - prepared gels.

incorporates into the network to form Si - O - B links, but not B - O - B bonds [26].

The broadest and intensive band in both IR spectra is observed at about 1100 cm^{-1} that is ascribed to the asymmetric stretching vibrations (ν_{as}) of SiO_4 groups and it is typical for a polymerized silica network [27]. The other absorption band registered in both spectra is that at 1200 cm^{-1}. Generally, it could be ascribed to the asymmetric Si - O stretching vibrations [28]. Having in mind the fact that it becomes more pronounced in the spectrum with higher B_2O_3 content (sample 80Si/B/Eu), it could be suggesting that this band is also related to the ν_{as} of BO_3 structural units [29].

Finally, the last two absorption bands are at 1500

and 1400 cm^{-1} but the first one appeared only in the IR spectrum of 80Si/B/Eu sample. These bands may be attributed to the asymmetric B - O stretching vibrations of trigonal BO_3 units [30]. However, the absence of a distinct band near ~ 870 cm^{-1} makes the clear confirmation of BO_3 groups difficult.

Luminescent emission spectra

Fig. 6 shows the photoluminescence emission spectra of Eu^{3+}: SiO_2 - B_2O_3 sol - gel glasses. A broad defect - related emission from the glass network and the characteristic sharp 4f - 4f transitions of Eu^{3+} ions were observed. Five emission bands are well - resolved and clearly seen at 500, 550, 600, 620 and 700 nm which is consistent with previous studies on Eu^{3+} - doped silica - borate glasses [31, 32]. The peaks at ~ 600 and ~ 620 nm correspond to the $^5D_0 \rightarrow {}^07F_1$ and $^5D_0 \rightarrow {}^7F_2$ transitions, respectively, while the weaker features near 550 and 700 nm originated from the $^5D_1 \rightarrow {}^7F_1$ and $^5D_0 \rightarrow {}^7F_4$ transitions. The peak at 620 nm is assigned to the $^5D_0 \rightarrow {}^7F_2$ transition and it dominated the spectrum in the sample containing higher SiO_2 amount (90 mol %). Obviously, the $^5D_0 \rightarrow {}^7F_2$ transition exceeded the intensity of the magnetic - dipole - allowed $^5D_0 \rightarrow {}^7F_1$ transition. This behaviour indicates that Eu^{3+} ions preferentially occupy non - centrosymmetric, highly distorted sites within the glass network, a structural characteristic typical for borosilicate systems where B_2O_3 increases disorder and covalence around rare - earth ions [33].

In the near - infrared region, a broad band centered around 1000 nm is observed which is stronger in the sample containing 80 mol % SiO_2. This feature could be attributed to the intrinsic structural defects of the silicate - borate matrix [34, 35]. Overall, the spectrum confirms successful incorporation of Eu^{3+} into the glass matrix

There is a peculiarity observed in the spectra of the investigated samples. This is related with the observation that the $^5D_0 \rightarrow {}^7F_1$ (~ 600 nm) and $^5D_0 \rightarrow {}^7F_2$ (~ 620 nm) emission bands exhibit comparable intensities. This phenomenon is observed in limited number of investigations [36 - 38]. In such disordered glass matrices, Eu^{3+} ions often occupy a distribution of local environments with varying degrees of site symmetry. Magnetic - dipole transitions like $^5D_0 \rightarrow {}^7F_1$ are largely insensitive to local symmetry, whereas the electric - dipole $^5D_0 \rightarrow {}^7F_2$ transition is hypersensitive to asymmetry. Comparable intensities of these two bands suggest that a significant fraction of Eu^{3+} ions reside in sites with different surround due to the present of small amount of H_3BO_3 (detected by the XRD analysis, Fig. 2) in the silica - borate amorphous matrix. This means that europium ions take a place of symmetric and asymmetric coordination [36 - 38].

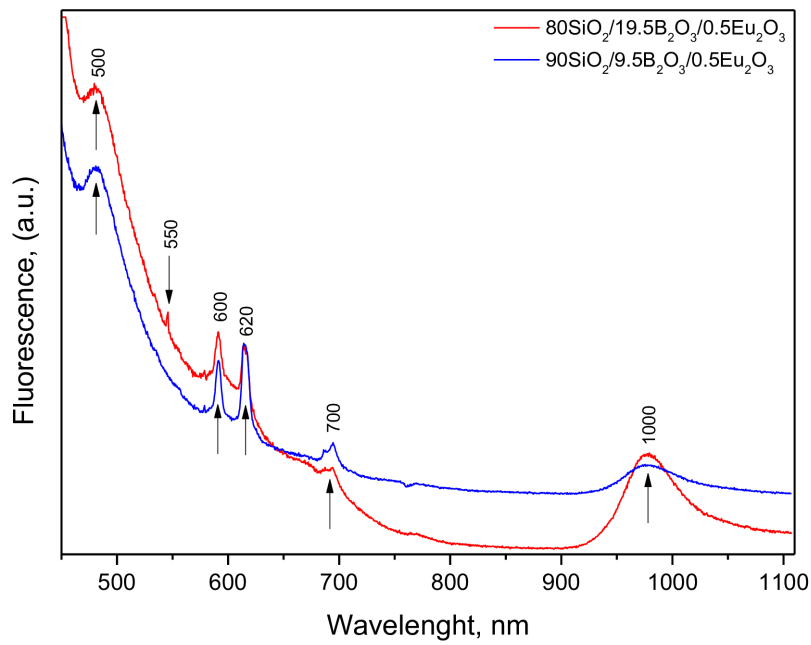

Fig. 6. Emission spectra of 90Si/B/Eu and 80Si/B/Eu excited at λ_{ex} = 385 nm.

CONCLUSIONS

Eu^{3+} doped glasses from the SiO_2 - B_2O_3 were prepared by the sol - gel method and their morphology, thermal stability, and structural characteristics were investigated. Transparent, monolithic gels containing B_2O_3 content up to 10 mol % were obtained. DTA analysis exhibited that the higher Eu^{3+} amount increased the thermal stability of the silica matrix. The optical microscope observations proved that the obtained samples are glasses. The IR spectra showed vibrations of SiO_4 and BO_3 structural groups. The luminescence spectrum shows successful incorporation of Eu^{3+} into the glass matrix. The two main Eu^{3+} emission bands at ~ 600 nm ($^5D_0 \rightarrow {}^7F_1$) and ~ 620 nm ($^5D_0 \rightarrow {}^7F_2$) with comparable intensity, indicated that Eu^{3+} ions occupy a range of local environments with intermediate symmetry in the glass.

Acknowledgments

The authors are thankful to the "National Center of Excellence Mechatronics and Clean Technologies" for the experimental work supported by the European Regional Development Fund under the "Research Innovation and Digitization for Smart Transformation" program 2021 - 2027. The research equipment used was from the distributed research infrastructure INFRAMAT, which was supported by the Bulgarian Ministry of Education and Science under contract.

Authors' contributions

A.B. - N., L. A.: Conceptualization, A.B. - N., L. A.: Methodology, H.L.: Investigation, A.B. - N., L.A., H.L.: Writing - Original draft preparation, A.B. - N., D.M., H.L.: Writing - Review and editing.

REFERENCES

1. C.J. Brinker, G.W. Scherer, Introduction to Sol-Gel Processing; Springer: Boston, MA, USA, 1990, ISBN 978-0-306-47689-1.
2. S. Esposito, Traditional Sol-Gel Chemistry as a Powerful Tool for the Preparation of Supported Metal and Metal Oxide Catalysts, Materials, 12, 2019, 668-678. https://doi.org/10.3390/ma12040668.
3. C.J. Brinker, G. Scherer, Sol-Gel Science: The Physics and Chemistry of Sol-Gel Processing, 1st ed.; Academic Press Inc, New York, NY, USA, 1990.
4. D. Levy, M. Zayat, The Sol-Gel Handbook: Synthesis, Characterization and Applications; Wiley-VCH, Weinheim, Germany, 2015.
5. A.E. Danks, S.R. Hall, Z. Schnepp, The evolution of „sol-gel"chemistry as a technique for materials synthesis, Mater. Horiz., 3, 2016, 91-112.
6. K. Deshmukh, T. Kovarik, T. Krenek, D. Docheva, T. Stich, J. Pola, Recent advances and future perspectives of sol-gel derived porous bioactive glasses: a review, RSC Adv., 56, 2020, 33835.
7. Y. Dimitriev, Y. Ivanova, R. Iordanova, History of sol-gel science and technology (review), JCTM, 2, 2008, 181-192.
8. J. Livage, F. Babonneau, C. Sanchez, Sol-Gel Chemistry for Optical Materials, Springer Int. Ser. Eng. Comput. Sci., 259, 1994, 39-58. https://doi.org/10.1007/978-1-4615-2750-3_2.
9. L. Hench, J. West, The sol-gel process, Chem. Rev., 90, 1, 1990, 33-68. https://pubs.acs.org/doi/10.1021/cr00099a003.
10. S. Choudhury, A review of the sol-gel process and its application, Int. J. Eng. Res., 10, 7, 2024, 122-125.
11. S. Sakka, The Current State of Sol-Gel Technology, J. Sol-Gel Sci. Technol., 3, 1994, 69-81.
12. J. del-Castillo, A.C. Yanes, J.J. Velazquez, J. Mendez-Ramos, V.D. Rodriguez, Luminescent properties of Eu^{3+}-Tb^{3+}-doped SiO_2-SnO_2-based nano-glass-ceramics prepared by sol-gel method, J. Alloys Compd., 473, 1-2, 2009, 571-575.
13. T. Hayakawa, M. Hayakawa, M. Nogami, Estimation of the fs laser spot temperature inside TeO_2-ZnO-Nb_2O_5 glass by using up-conversion green fluorescence of Er^{3+} ions, J. Alloys Compd., 451, 1-2, 2008, 77-80.
14. M.S. Shakeri, M. Rezvani, Optical band gap and spectroscopic study of lithium alumino silicate glass containing Y^{3+} ions, Spectrochim. Acta A Mol. Biomol. Spectrosc., 79, 5, 2011, 1920-1925.
15. G. Pedroza, W.M. de Azevedo, H.J. Khoury, E.F. da Silva Jr., Gamma ray detection using sol-gel Glass doped with lanthanide ions, Appl. Radiat. Isot., 56, 3, 2002, 563-566.
16. P. Yang, C. Feng Song, M. Kai Lu, J. Chang, Y. Zi Wang, Z. Xi Yang, G. Jun Zhou, Z. Ping Ai, D. Xu, D. Long Yuan, Defects and Photoluminescence of

Ni^{2+} and Mn^{2+}-Doped Sol-Gel SiO_2 Glass, J. Solid State Chem., 160, 2001, 272-277.
17. B. Kumar, Sol-gel processing of SiO_2-B_2O_3 glasses, Mat. Res. Bull., 19, 1984, 331-338.
18. X. Zhao, X.D. He, S. Zhang, L.D. Wang, M.W. Li, Y.B. Li, Investigations on B-doped SiO_2 thermal protective coatings by hybrid sol-gel method, Thin Solid Films, 519, 2011, 4849-4854.
19. E.I. Kamitsos, Infrared-reflectance spectra of heat-treated, sol-gel-derived silica, Phys. Rev. B, 53, 1996, 14662.
20. E.I. Kamitsos, A.P. Patsis, G. Kordas, Infrared-reflectance spectra of heat-treated, sol-gel-derived silica, Phys. Rev. B, 48, 17, 1993, 12499-12506.
21. A. Shalaby, T. Angelova, A. Bachvarova-Nedelcheva, N. Georgieva, R. Iordanova, A. Staneva, Y. Dimitriev, Sol-gel synthesis of materials in the system SiO_2/ZnO/TiO_2/RGO and their antimicrobial efficiency against E. Coli K12, C. R. Acad. Bulg. Sci., 9, 1, 2016, 25-30.
22. N. Rangelova, L. Aleksandrov, S. Nenkova, Synthesis and characterization of pectin/SiO_2 hybrid materials, J. Sol-Gel Sci. Technol., 85, 2018, 330-339.
23. J.L. Parsons, M.E. Milberg, Vibrational Spectra of Vitreous $B_2O_3xH_2O$, J. Am. Ceram. Soc., 43, 6, 1960, 326-330.
24. D.E. Bethell, N. Sheppard, The infra-red spectrum and structure of boric acid, Trans. Faraday Soc., 51, 1955, 9-15.
25. R. Jabra, J. Phalippou, J. Zarzycki, Synthesis of binary glass-forming oxide glasses by hot-pressing of gels, J. Non-Cryst. Solids., 42, 1-3, 1980, 489-498.
26. M. Nogami, Y. Moriya, Glass formation of the SiO_2-B_2O_3 system by the gel process from metal alkoxides, J. Non-Cryst. Solids., 48, 2-3, 1982, 359-366.
27. I. Plusnina, Infrared spectra of silicates; Moscow Univ. Publ, Moscow (1967), (in Russian).
28. B. Ritzer, M.A. Villegas, J.M. Fernández Navarro, Influence of temperature and time on the stability of silver in silica sol-gel glasses, J. Sol-Gel Sci. Technol., 8, 1997, 917-921.
29. Y. Lai, Y. Zeng, X. Tang, H. Zhang, J. Han, H. Su, Structural investigation of calcium borosilicate glasses with varying Si/Ca ratios by infrared and Raman spectroscopy, RSC Adv., 6, 2016, 93722-93728.
30. H. Doweidar, G. El-Damrawi, M. Abdelghany, Structure and properties of CaF_2-B_2O_3 glasses, J. Mater. Sci., 47, 9, 4028-4035.
31. S. Rakpanich, N. Wantana, Y. Ruangtaweep, J. Kaewkhao, Eu^{3+} doped Borosilicate Glass for Solid-State Luminescence Material, J. Met. Mater. Miner., 27, 1, 2017, 35-38.
32. Y. Gong, L. Li, J. Chen, H. Guo, Photoluminescent and Scintillating Performance of Eu^{3+}-Doped Boroaluminosilicate Glass Scintillators, Materials, 2023, 16, 2023, 4711.
33. B. Damdee, K. Kirdsiri, J. Kaewkhao, Properties and Investigation on effect of Eu^{3+} Ions in Lithium Barium Borate Glasses, Key Eng. Mater., 675-676, 2016, 380-383.
34. S.F. Abdul Sani, A.A.Z. Ahmad Nazeri, M.F. Mohd Zainal, K.S. Almugren, S.N. Sabtu, D.A. Bradley, Dual radiation characterization of borosilicate glass slides: Thermoluminescence response to neutrons and optical properties under gamma irradiation, Phys. Open, 25, 2025, 100309.
35. J. Fournier, J. Néauport, P. Grua, V. Jubera, E. Fargin, D. Talaga, S. Jouannigot, Luminescence study of defects in silica glasses under near-UV excitation, Phys. Procedia, 8, 2010, 39-43.
36. B. Bondzior, T. Hoang, T.H. Quan Vu, P.J. Deren, L. Petit, Unveiling the thermometric sensitivity of Eu^{3+}doped glasses in various system from theory to experimental, SSRN Electronic Journal, 227, 2023, 115310-115315.
37. M.A. Cherbib, S. Kapoor, M. Bockowski, M.M. Smedskjaer, L. Wondraczek, Luminescence behaviour of Eu^{3+} in hot-compressed silicate glasses, J. Non-Cryst. Solids: X, 4, 2019, 100041-100047.
38. A. Hernández, M. de León Alfaro, A. Villatoro, C. Falcony, T. Montalvo, J. Medina, Luminescence Characteristics of $LaAlO_3$:Eu^{3+} Obtained by Modified Pechini's Method, Open J. Synth. Theory Appl., 6, 2017, 1-12.